J. Phys. B: At. Mol. Opt. Phys. **31** (1998) 4833–4852. Printed in the UK PII: S0953-4075(98)90362-5

Electron impact excitation of the $np^5(n+1)p$ states of Ar ($n=3$), Kr ($n=4$) and Xe ($n=5$) atoms

Savinder Kaur†, R Srivastava†, R P McEachran‡§ and A D Stauffer‡

† Department of Physics, University of Roorkee, Roorkee 247667, India

‡ Department of Physics and Astronomy, York University, Toronto, Canada M3J 1P3

Received 6 January 1998, in final form 21 July 1998

Abstract. Electron impact excitation of all the $np^5(n+1)p$ $J=1,2$ and 3 states of argon ($n=3$), krypton ($n=4$) and xenon ($n=5$) from the ground np^6 $J=0$ state has been considered in the relativistic distorted-wave approximation. The differential and total cross sections are obtained for incident electrons in the energy range from 15 to 100 eV. The results are compared with the available experimental data and a few theoretical non-relativistic and semi-relativistic calculations wherever possible.

1. Introduction

In our previous paper (Kaur *et al* 1998, hereafter referred to as I), we presented the relativistic distorted-wave (RDW) calculations for the electron impact excitation of all the $2p^53p$ $J=1,2$ and 3 states of neon from the ground $2p^6$ $J=0$ state. We reported results for the differential cross sections (DCS) and the differential Stokes parameters P_i, $i=1$ to 4, of the decay of the different excited states by photon emission to the various $2p^53s$ states. In the present paper we have extended this work to the corresponding np^6 $J=0 \rightarrow np^5(n+1)p$ $J=1,2$ and 3 excitations in other inert gases, namely argon ($n=3$), krypton ($n=4$) and xenon ($n=5$). In paper I an introduction to the study of such states in the inert gases was given, as were the details of the RDW theory. These results also apply to the present paper and will not be repeated here.

In neon most previous experimental and theoretical work involved the Stokes parameters and not the values of the cross sections. On the other hand, for the corresponding higher-lying $np^5n'l$ excited states in argon, krypton and xenon, it is mostly the DCS and total cross section (TCS) which have been reported in the literature. We therefore confine ourselves to the study of cross sections in the present paper. For argon experimental results have been given by Ballou *et al* (1973), Bogdanova and Yurgenson (1987), Gay *et al* (1996) and Chilton *et al* (1998) for the TCS and by Chutjian and Cartwright (1981) for the DCS. The theoretical calculations for argon are the non-relativistic distorted-wave (DWA) results for the TCS by Bubelev and Grum-Grzhimailo (1991), the semi-relativistic distorted-wave (SRDW) results by Madison *et al* (1998) and the semi-relativistic *R*-matrix results by Zeman and Bartschat (private communication) for the DCS and TCS. In the case of krypton, only Trajmar *et al* (1981) have reported experimental DCS and TCS results for a few transitions and there are no theoretical calculations available. However, for some of the unresolved

§ Current address: Electron Physics Group, Atomic and Molecular Physics Laboratories, Australian National University, Canberra, ACT 0200, Australia.

0953-4075/98/214833+20$19.50

excitations in xenon, experimental DCS were reported by Ester and Kessler (1994), Filipović *et al* (1988) and recently by Khakoo *et al* (1996). Along with their experimental data, Khakoo *et al* (1996) also presented non-relativistic DWA and first-order many-body theory (FOMBT) calculations. Recently, Nakazaki *et al* (1997) also carried out semi-relativistic R-matrix calculations in order to compare with these experimental results at low energies. The available literature clearly indicates that for an understanding of such excitations and for comparison with the various experimental cross section data available, there is a need of a systematic theoretical investigation of the problem. In this paper we have therefore carried out RDW calculations for all the excited $n\mathrm{p}^5(n+1)\mathrm{p}$ $J = 1, 2$ and 3 states of argon ($n = 3$), krypton ($n = 4$) and xenon ($n = 5$) from the $n\mathrm{p}^6$ $J = 0$ state and report complete set of results for the DCS and TCS at selected energies.

2. Target wavefunctions

In terms of the relativistic atomic structure description of Grant (1970), the configuration of the ground state can be represented by $n\bar{\mathrm{p}}^2 n\mathrm{p}^4$ and the excited states by $(n\bar{\mathrm{p}})^2(n\mathrm{p})^3(n+1)j$ or $(n\bar{\mathrm{p}})(n\mathrm{p})^4(n+1)j$. Here all the inner subshells (1s–ns) are full and are therefore not specified. Also the excited $(n+1)j$ orbital can be either $(n+1)\bar{\mathrm{p}}$ or $(n+1)\mathrm{p}$ in the present context. For the transition $a \to b$ we let ϕ_a and ϕ_b represent the ground and excited states which, in turn, can be constructed from the Dirac–Fock determinants.

The configurations of interest in this paper can be represented by the outer two or three orbitals along with the value of J, the total angular momentum of the atom. The ground state of these three noble gases is therefore given by

$$\phi_a = \left(n\bar{\mathrm{p}}^2 n\mathrm{p}^4\right)_{J_a=0} \tag{1}$$

while the excited states, corresponding to different J values, are given by

$$\phi_b(J_b=1) = C_1\left(n\bar{\mathrm{p}}^2 n\mathrm{p}^3 m\bar{\mathrm{p}}\right)_{J_b=1} + C_2\left(n\bar{\mathrm{p}} n\mathrm{p}^4 m\mathrm{p}\right)_{J_b=1} + C_3\left(n\bar{\mathrm{p}}^2 n\mathrm{p}^3 m\mathrm{p}\right)_{J_b=1} + C_4\left(n\bar{\mathrm{p}} n\mathrm{p}^4 m\bar{\mathrm{p}}\right)_{J_b=1} \tag{2a}$$

$$\phi_b(J_b=2) = C_1\left(n\bar{\mathrm{p}}^2 n\mathrm{p}^3 m\bar{\mathrm{p}}\right)_{J_b=2} + C_2\left(n\bar{\mathrm{p}} n\mathrm{p}^4 m\mathrm{p}\right)_{J_b=2} + C_3\left(n\bar{\mathrm{p}}^2 n\mathrm{p}^3 m\mathrm{p}\right)_{J_b=2} \tag{2b}$$

and

$$\phi_b(J_b=3) = \left(n\bar{\mathrm{p}}^2 n\mathrm{p}^3 m\mathrm{p}\right)_{J_b=3} \tag{2c}$$

where $m = n+1$. As in paper I, there are four excited states for $J_b = 1$, i.e. $m\mathrm{p}\left[\frac{1}{2}\right]_1$, $m\mathrm{p}\left[\frac{3}{2}\right]_1$, $m\mathrm{p}'\left[\frac{3}{2}\right]_1$ and $m\mathrm{p}'\left[\frac{1}{2}\right]_1$ using the spectroscopic notation of Moore (1971) with configuration mixing coefficients C_1 to C_4 for argon ($m = 4$), krypton ($m = 5$) and xenon ($m = 6$). Similarly, for $J_b = 2$ there are three excited states, namely $m\mathrm{p}\left[\frac{5}{2}\right]_2$, $m\mathrm{p}\left[\frac{3}{2}\right]_2$ and $m\mathrm{p}'\left[\frac{3}{2}\right]_2$ with corresponding mixing coefficients, while for $J_b = 3$ there is only the one $m\mathrm{p}\left[\frac{5}{2}\right]_3$ state. The radial wavefunctions and the configuration mixing coefficients were obtained using the relativistic multi-configuration Dirac–Fock (MCDF) program of Grant *et al* (1980). The mixing coefficients for the various $J_b = 1$ and $J_b = 2$ states are given in table 1. We note from this table that the various excited states are dominated by a single j–j coupled configuration with the exception of the $m\mathrm{p}\left[\frac{1}{2}\right]_1$ and $m\mathrm{p}\left[\frac{3}{2}\right]_1$ states. This domination becomes almost complete for the heaviest target, xenon.

We have also assessed the importance of correlation effects in the description of the ground-state wavefunction by representing it as

$$\phi_a(J_a=0) = a_1\left(n\bar{\mathrm{p}}^2 n\mathrm{p}^4\right)_{J_a=0} + a_2\left(n\bar{\mathrm{p}} n\mathrm{p}^4 m\bar{\mathrm{p}}\right)_{J_a=0} + a_3\left(n\bar{\mathrm{p}}^2 n\mathrm{p}^3 m\mathrm{p}\right)_{J_a=0}. \tag{3}$$

Table 1. Values of the configuration mixing coefficients C_1, C_2, C_3 and C_4 corresponding to the different excited states $np^5(n+1)p$, $J_b = 1, 2$ and 3 of Ar, Kr and Xe for the SCGS wavefunctions in equation (1).

Atom	J_b	Excited state	C_1	C_2	C_3	C_4
Ar	1	$4p[1/2]_1$	0.624 447 46	−0.359 045 25	−0.681 768 83	0.127 840 34
$n = 3$		$4p[3/2]_1$	−0.691 392 76	0.110 212 17	−0.627 377 02	0.340 921 42
		$4p'[3/2]_1$	−0.257 625 72	−0.290 683 97	−0.249 229 98	−0.887 139 36
		$4p'[1/2]_1$	−0.256 262 41	−0.880 024 22	0.281 910 91	0.283 572 21
	2	$4p[5/2]_2$	−0.959 274 89	−0.156 444 10	−0.235 195 53	
		$4p[3/2]_2$	−0.195 887 64	−0.231 467 53	0.952 917 00	
		$4p'[3/2]_2$	0.203 518 37	−0.960 181 25	−0.191 395 52	
Kr	1	$5p[1/2]_1$	0.692 003 33	−0.168 463 27	−0.699 520 20	0.058 506 57
$n = 4$		$5p[3/2]_1$	−0.709 913 49	0.016 385 67	−0.699 543 59	0.079 956 98
		$5p'[3/2]_1$	0.039 223 06	0.183 853 76	0.076 422 55	0.979 193 00
		$5p'[1/2]_1$	−0.124 963 15	−0.968 271 36	0.124 377 88	0.177 101 45
	2	$5p[5/2]_2$	0.966 788 25	0.044 364 08	0.251 698 83	
		$5p[3/2]_2$	0.249 246 54	0.054 200 49	−0.966 922 16	
		$5p'[3/2]_2$	0.056 538 82	−0.997 544 05	−0.041 342 80	
Xe	1	$6p[1/2]_1$	0.742 811 62	−0.096 195 79	−0.661 800 09	0.031 589 57
$n = 5$		$6p[3/2]_1$	−0.665 510 84	0.001 606 72	−0.745 214 16	0.041 816 12
		$6p'[3/2]_1$	0.009 716 87	0.076 184 41	0.047 370 62	0.995 920 45
		$6p'[1/2]_1$	−0.072 331 10	−0.992 441 29	0.066 577 17	0.073 457 26
	2	$6p[5/2]_2$	0.974 627 11	0.022 735 12	0.222 677 13	
		$6p[3/2]_2$	0.222 073 90	0.026 323 31	−0.974 674 44	
		$6p'[3/2]_2$	0.028 020 94	−0.999 394 92	−0.020 606 54	

These multi-configuration wavefunctions for the ground states of Ar, Kr and Xe were also obtained using the MCDF program of Grant *et al* (1980). The corresponding mixing coefficients which were obtained are given by $a_1 = -0.988\,304\,41$, $a_2 = 0.087\,940\,17$ and $a_3 = 0.124\,582\,98$ for argon, $a_1 = 0.989\,331\,80$, $a_2 = -0.080\,749\,12$ and $a_3 = -0.121\,252\,49$ for krypton and $a_1 = -0.989\,961\,94$, $a_2 = 0.073\,500\,69$ and $a_3 = 0.120\,718\,71$ for xenon. Furthermore, corresponding to this multi-configuration ground-state wavefunction, new excited-state wavefunctions were also determined. The new values for the mixing coefficients are given in table 2. Thus, in this paper, we report two sets of calculations, one using the single-configuration ground-state (SCGS) wavefunction (equation (1)) and the other using the multi-configuration ground-state (MCGS) wavefunction, as given in equation (3), for all the transitions considered.

It is instructive to consider the representation of the various excited states in LS coupling. The $J_b = 1$ states are mixtures of ^{1}P, ^{3}S, ^{3}P and ^{3}D configurations, the $J_b = 2$ states are mixtures of ^{1}D, ^{3}P and ^{3}D configurations, while the $J_b = 3$ state is a pure ^{3}D configuration. Thus excitation of the $\left[\frac{5}{2}\right]_3$ state can proceed only via an electron exchange reaction, while excitation of the $J_b = 2$ states can be accomplished by direct as well as exchange excitation because of the admixture of the $^1D_2$ configuration. It would similarly appear that the presence of the $^1P_1$ configuration in the $J_b = 1$ states would allow for a direct excitation of these states, but in fact the direct matrix elements for these transitions are zero in the RDW approximation.

Table 2. Values of the configuration mixing coefficients C_1, C_2, C_3 and C_4 corresponding to the different excited states $np^5(n+1)p$, $J_b = 1, 2$ and 3 of Ar, Kr and Xe for the MCGS wavefunctions in equation (3).

Atom	J_b	Excited state	C_1	C_2	C_3	C_4
Ar	1	$4p[1/2]_1$	0.631 751 70	−0.343 541 05	−0.684 009 57	0.122 465 49
$n = 3$		$4p[3/2]_1$	−0.699 755 91	0.094 946 60	−0.639 601 66	0.303 704 68
		$4p'[3/2]_1$	−0.224 855 81	−0.286 490 68	−0.225 580 84	−0.903 590 75
		$4p'[1/2]_1$	−0.246 315 50	−0.889 318 72	0.268 614 80	0.276 200 97
	2	$4p[5/2]_2$	−0.956 260 15	−0.124 847 86	−0.264 536 46	
		$4p[3/2]_2$	−0.233 070 96	−0.221 279 09	0.946 949 57	
		$4p'[3/2]_2$	−0.176 761 02	0.967 185 90	0.182 501 97	
Kr	1	$5p[1/2]_1$	0.698 837 18	−0.156 391 28	−0.695 879 62	0.054 036 26
$n = 4$		$5p[3/2]_1$	0.704 980 47	−0.013 476 71	0.705 354 42	−0.072 774 04
		$5p'[3/2]_1$	0.032 675 98	0.165 616 73	0.071 927 58	0.983 020 75
		$5p'[1/2]_1$	0.116 453 49	0.973 617 61	−0.114 250 26	−0.159 543 78
	2	$5p[5/2]_2$	0.963 448 00	0.036 404 11	0.265 410 43	
		$5p[3/2]_2$	0.263 404 36	0.051 920 00	−0.963 287 32	
		$5p'[3/2]_2$	−0.048 847 73	0.997 987 50	0.040 433 22	
Xe	1	$6p[1/2]_1$	−0.751 013 40	0.089 184 56	0.653 594 44	−0.028 970 56
$n = 5$		$6p[3/2]_1$	−0.656 812 90	0.000 462 56	−0.753 056 94	0.048 753 62
		$6p'[3/2]_1$	0.008 005 21	0.066 147 63	0.044 355 14	0.996 791 37
		$6p'[1/2]_1$	0.067 168 45	0.993 816 08	−0.061 254 98	−0.063 763 90
	2	$6p[5/2]_2$	0.973 103 63	0.019 233 57	0.229 563 49	
		$6p[3/2]_2$	0.229 057 12	0.025 366 27	−0.973 082 42	
		$6p'[3/2]_2$	−0.024 539 02	0.999 493 18	0.020 278 43	

3. Results and discussion

For the excitation of the various $J_b = 1, 2$ and 3 states from the ground $J_a = 0$ state, the T-matrix elements were calculated using the RDW method as described in paper I. The differential and total cross sections were then obtained in the usual manner at incident electron energies where experimental measurements are available for comparison. Where no experimental data or theoretical calculations are available, we present our DCS results graphically at 50 and 100 eV only, while the TCS results are given in tabular form for some selected energies. We compare both our SCGS and MCGS calculations with theory and experiment wherever available for Ar, Kr and Xe.

3.1. Differential cross sections

3.1.1. Argon. Our RDW results for the DCS for argon are shown in figures 1–4 and are compared with the experimental cross sections of Chutjian and Cartwright (1981). They measured the DCS in the angular range 5–138° and then extrapolated these results to both forward and backward scattering angles. They also put their DCS data on an absolute scale with respect to their earlier elastic scattering measurements. We also compare our cross sections with the SRDW theory of Madison *et al* (1998) at 30, 50 and 100 eV and with the semi-relativistic R-matrix calculation of Zeman and Bartschat (private communication) at 30 eV.

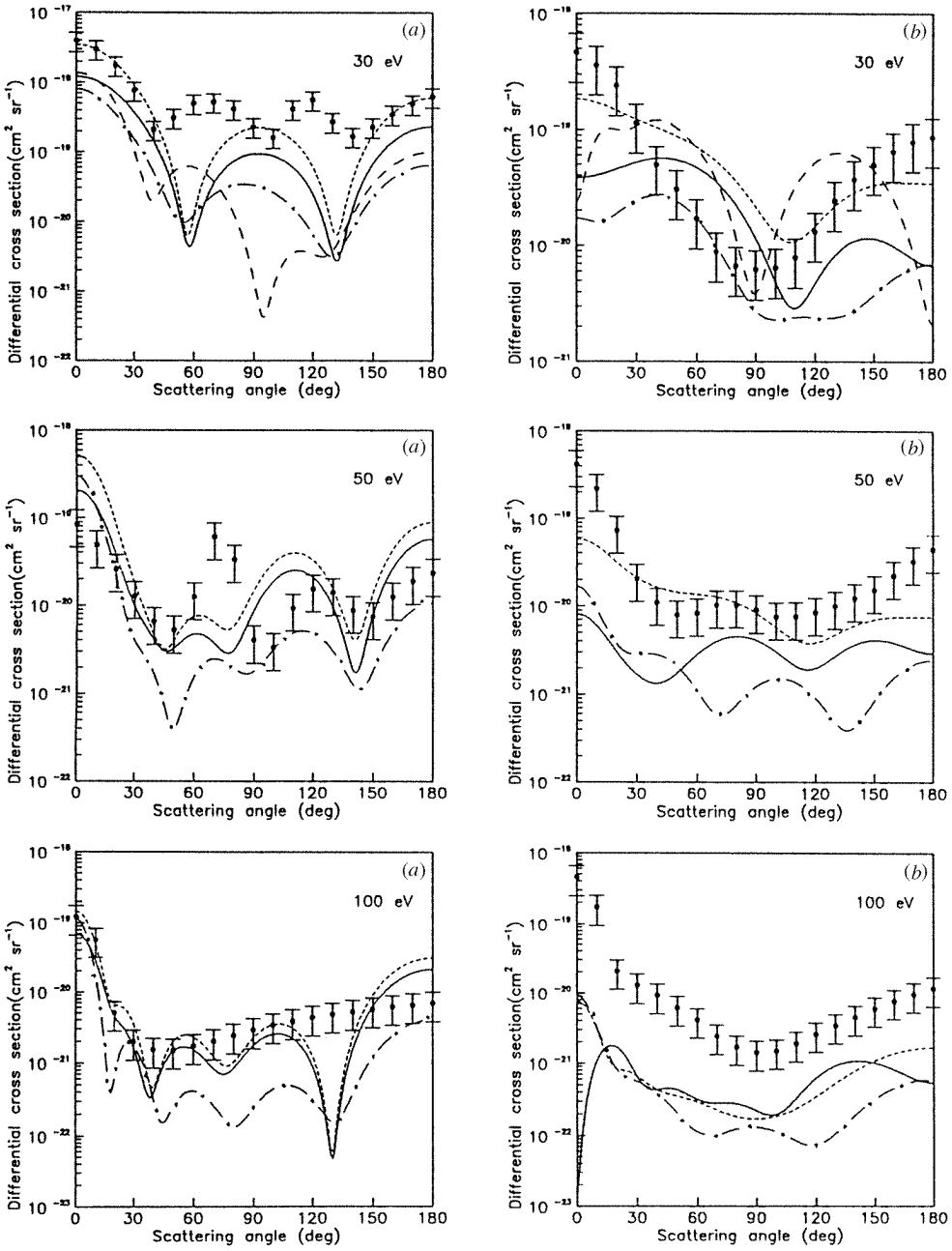

Figure 1. Comparison of the DCS with experiment for the excitation of Ar to (*a*) the $4p[\frac{1}{2}]_1$ state and (*b*) the $4p'[\frac{1}{2}]_1$ state at 30, 50 and 100 eV. Theory: ——, present SCGS results; — · —, present MCGS results; - - - -, SRDW results of Madison *et al* (1998). – – –, semi-relativistic *R*-matrix results of Zeman and Bartschat (private communication). Experiment: ●, Chutjian and Cartwright (1981).

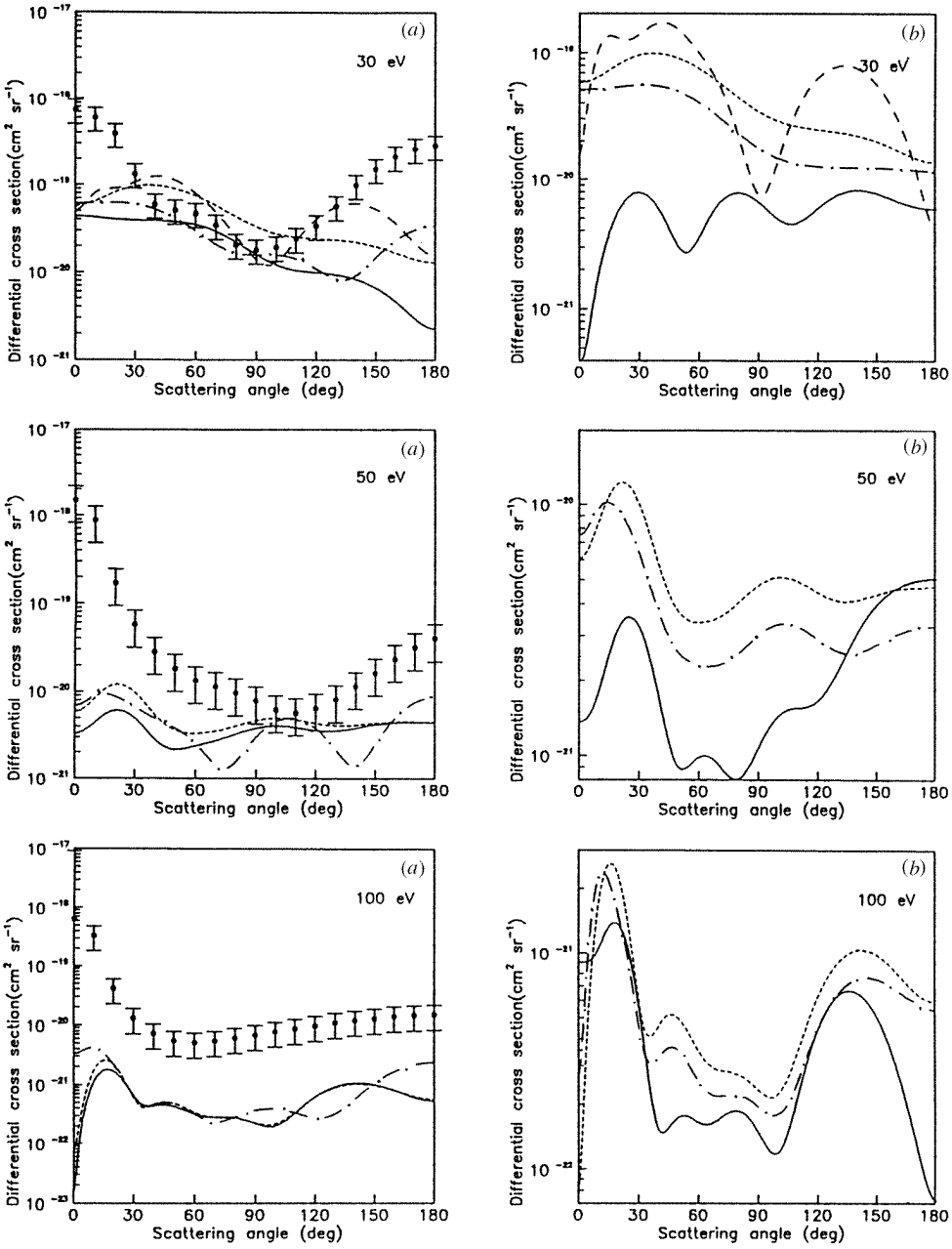

Figure 2. Same as figure 1 but for (*a*) the $4p\left[\frac{3}{2}\right]_1$ state and (*b*) the $4p'\left[\frac{3}{2}\right]_1$ state of Ar.

Figures 1 and 2 show the cross sections for the excitation of the $J_b = 1$ states. There is considerable variation among the different theoretical results for this transition and none of them show consistent agreement with experiment. For the most part, these cross sections exhibit the behaviour of transitions which proceed via an exchange reaction, namely a

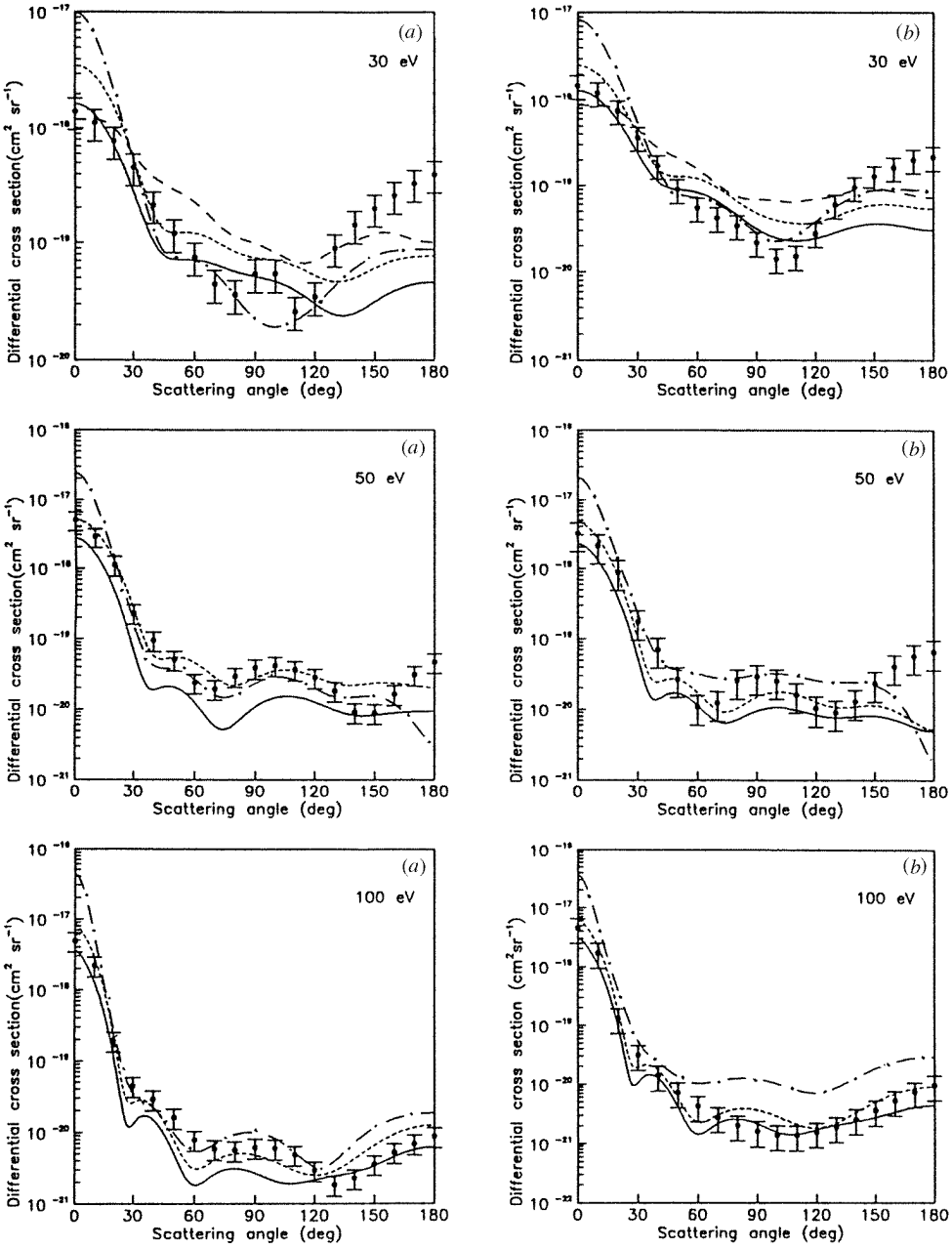

Figure 3. Same as figure 1 but for (*a*) the $4p\left[\frac{5}{2}\right]_2$ state and (*b*) the $4p'\left[\frac{3}{2}\right]_2$ state of Ar.

relatively flat cross section with the absence of the strong forward peak characteristic of spin-allowed transitions. The exception is the $4p\left[\frac{1}{2}\right]_1$ state where all the theories and the experiment predict such a forward peak and agree well in magnitude in this angular region. This is doubly surprising since this state is dominated by the ^{3}S configuration in *LS* coupling.

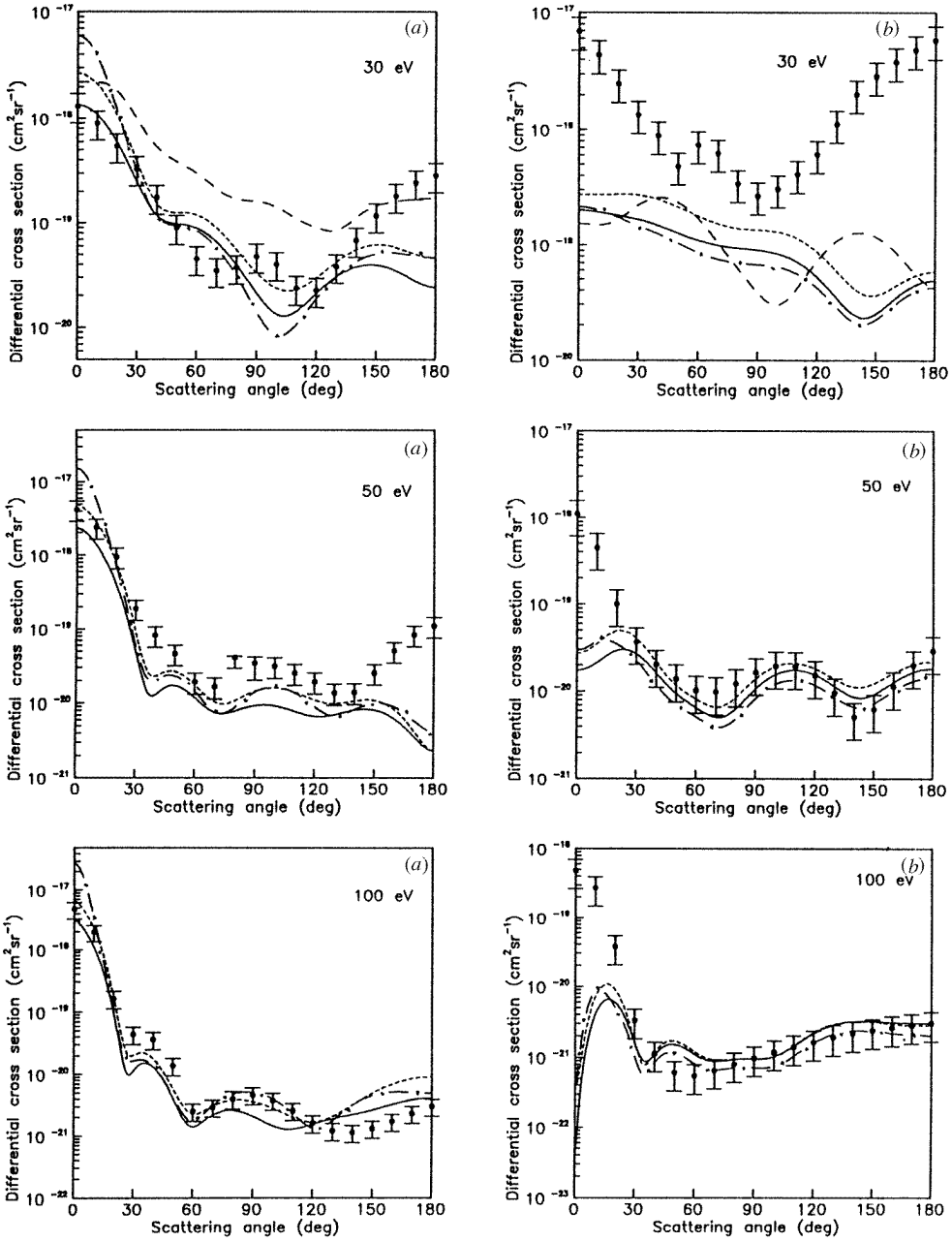

Figure 4. Same as figure 1 but for (*a*) the $4p[\frac{3}{2}]_2$ state and (*b*) the $4p[\frac{5}{2}]_3$ state of Ar.

Figures 3 and 4 contain our results for the excitation of the $J_b = 2$ and 3 states. As expected, the cross sections for the $J_b = 2$ states have the strong forward peak of a singlet–singlet transition, while those for the $J_b = 3$ state are relatively flat. There is good agreement between all the distorted-wave theories for these transitions, both in shape and

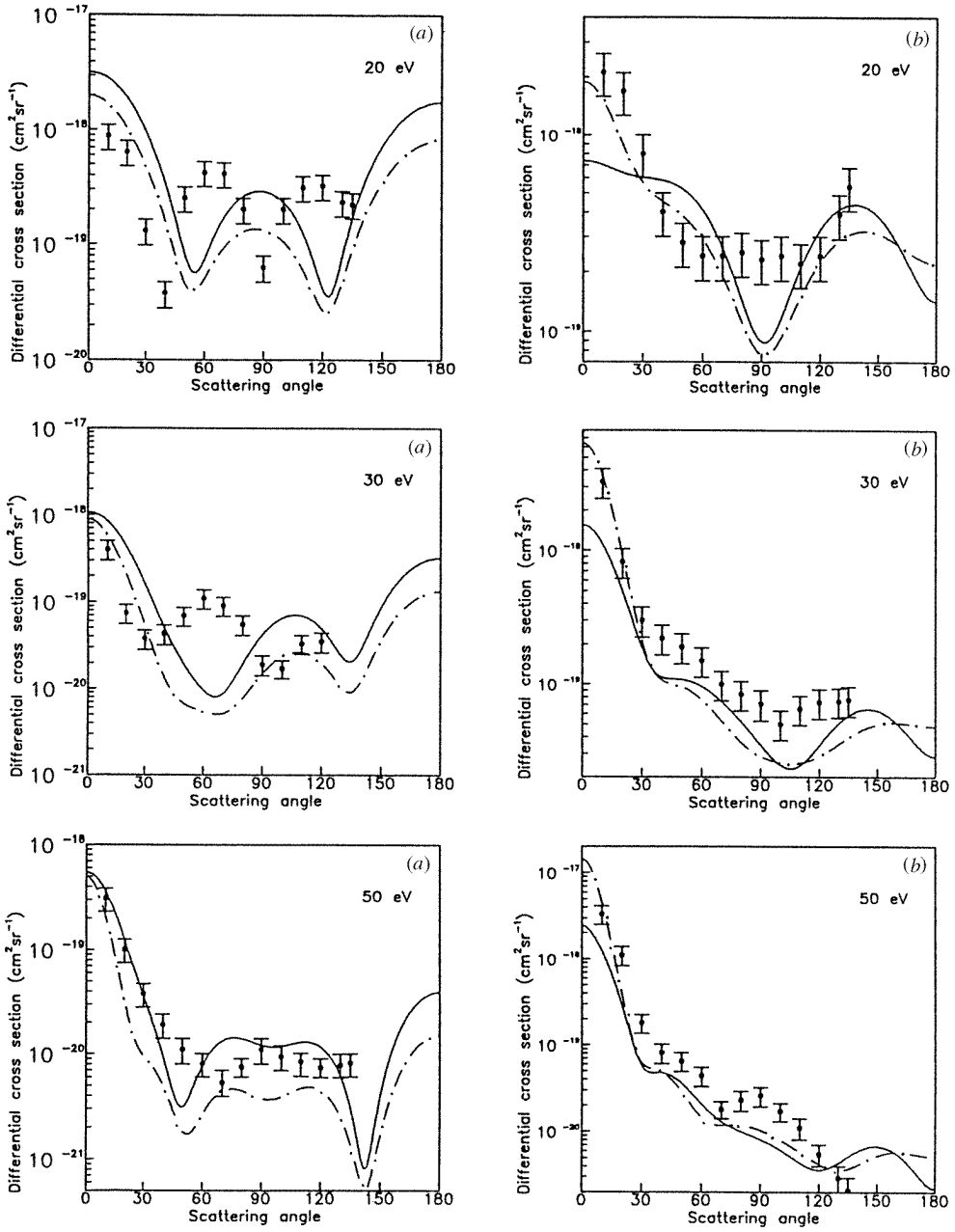

Figure 5. Comparison of the DCS with experiment for the excitation of Kr to (*a*) the $5p[\frac{1}{2}]_1$ state and (*b*) the unresolved $5p[\frac{3}{2}]_2 + 5p[\frac{3}{2}]_1$ states at 20, 30 and 50 eV. Theory: ——, present SCGS results; — · —, present MCGS results; experiment: ●, Trajmar *et al* (1981).

magnitude. There is also good agreement with the experimental measurements for all the $J_b = 2$ states. The agreement is less satisfactory for the $J_b = 3$ state, especially in the forward direction. We also note that cross sections for all the $J_b = 2$ states are very similar both in shape and magnitude.

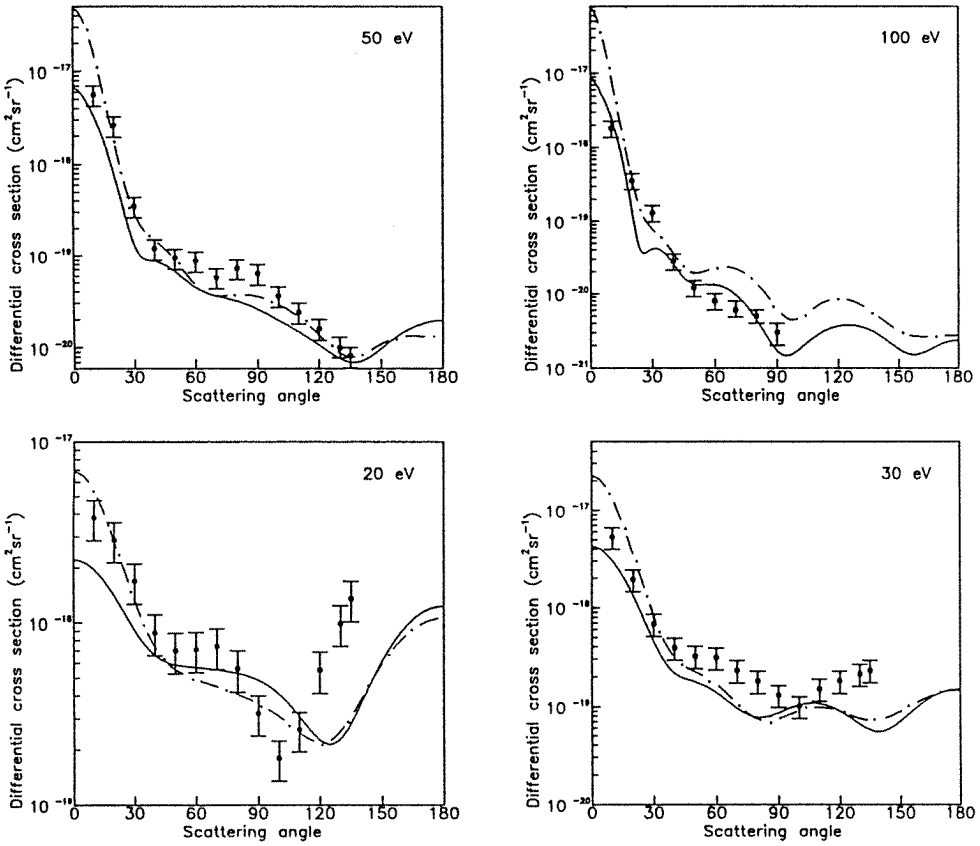

Figure 6. Same as figure 5 but for the unresolved $5p[\frac{5}{2}]_3 + 5p[\frac{5}{2}]_2$ states of Kr at 20, 30, 50 and 100 eV.

Although there is not consistent agreement between the experimental data and our RDW calculations, overall it appears that the SCGS results agree better with this data than the MCGS values, especially in the forward direction for the $J_b = 2$ states.

3.1.2. Krypton. For krypton the DCS results for various excitations of the $4p^5 5p$, $J_b = 1, 2$ and 3 states are shown in figures 5 and 6. In these figures we compare both our SCGS and MCGS results with the experimental data from Trajmar *et al* (1981) for a few selected transitions. They have reported DCS results in the angular range 5–135° and have normalized their data to an absolute scale with the help of the DCS for elastic scattering which, in turn, was normalized with respect to the DCS results for helium. In figures 5(*a*) and (*b*) we present DCS results for the $5p[\frac{1}{2}]_1$ state and for the combined unresolved $5p[\frac{3}{2}]_1 + 5p[\frac{3}{2}]_2$ states, respectively, and compare them with our RDW results at 20, 30 and 50 eV. In figure 6 we show the combined DCS results for the unresolved $5p[\frac{5}{2}]_2 + 5p[\frac{5}{2}]_3$ states at 20, 30, 50 and 100 eV. The behaviour of these cross sections is similar to that of the argon cross sections discussed above. In particular, the agreement with the experimental results is quite good except for the ones for the $J_b = 1$ state where there is some difference in shape though not in magnitude. However, for krypton, the MCGS

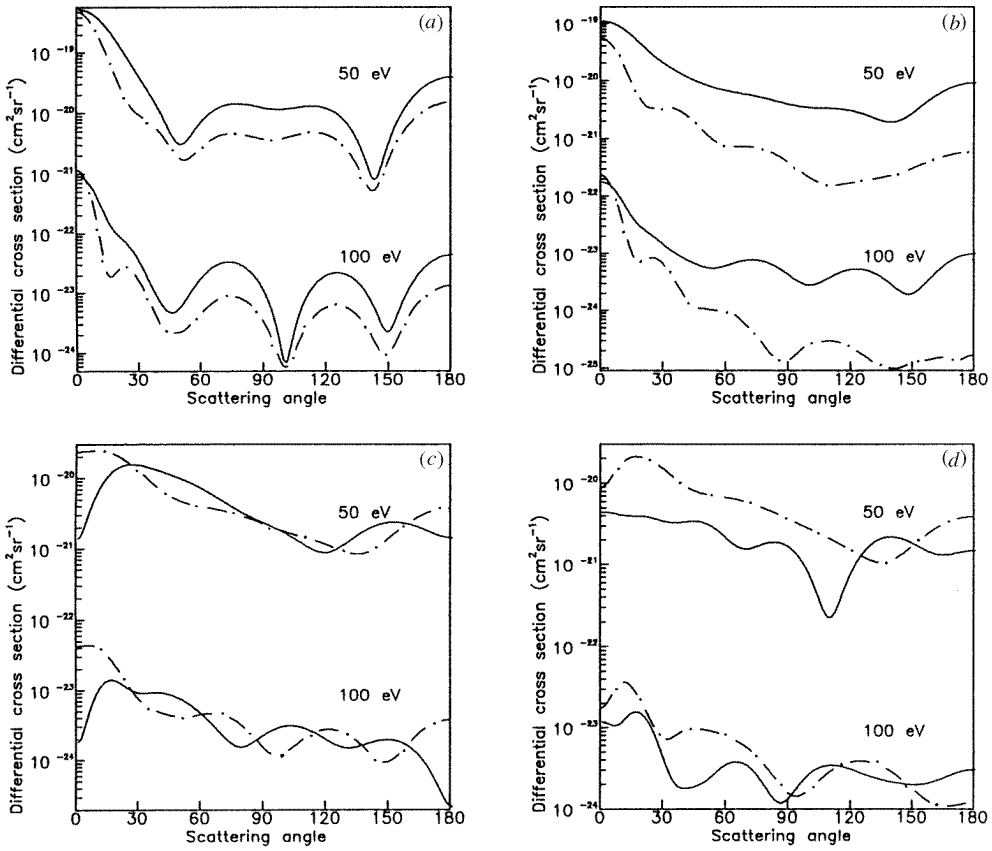

Figure 7. The DCS results for the excitation of different $4p^5 5p$ $J_b = 1$ states in Kr: (*a*) $5p[\frac{1}{2}]_1$, (*b*) $5p'[\frac{1}{2}]_1$, (*c*) $5p[\frac{3}{2}]_1$ and (*d*) $5p'[\frac{3}{2}]_1$. (Note that the values at 100 eV have been divided by 100.) Theory: ——, present SCGS results; — · —, present MCGS results.

results seem to be in better agreement with the experimental data than the SCGS results, contrary to our experience for argon. Since there are no experimental DCS data available for other states, we present, in figures 7 and 8, our SCGS and MCGS calculations for the DCS for all of the $J_b = 1, 2$ and 3 states at 50 and 100 eV. Again the behaviour of these cross sections is similar to that for the various states of argon.

3.1.3. Xenon. In figures 9–11 we present DCS results for the excitation of different $5p^5 6p$, $J_b = 1, 2$ and 3 states of xenon. The only experimental data available for these excitations are for the unresolved $6p[\frac{5}{2}]_2 + 6p[\frac{5}{2}]_3$ states and the $6p[\frac{3}{2}]_1 + 6p[\frac{3}{2}]_2$ states at 15, 20 and 30 eV and in the angular range 0–135° (Khakoo *et al* 1996) and 0–150° (Filipović *et al* 1988). They measured relative DCS values and put them on an absolute scale, with respect to the combined first two lowest excited states of xenon, which in turn, were normalized with the help of the elastic DCS measurements of Register *et al* (1986). Khakoo *et al* (1996) also reported non-relativistic DWA and FOMBT calculations and found the latter to be the more reliable. Consequently, we have included only their FOMBT calculations in our comparisons. We note that the manner in which the atomic wavefunctions are constructed in the FOMBT is equivalent to our MCGS method. We also compare with the semi-relativistic

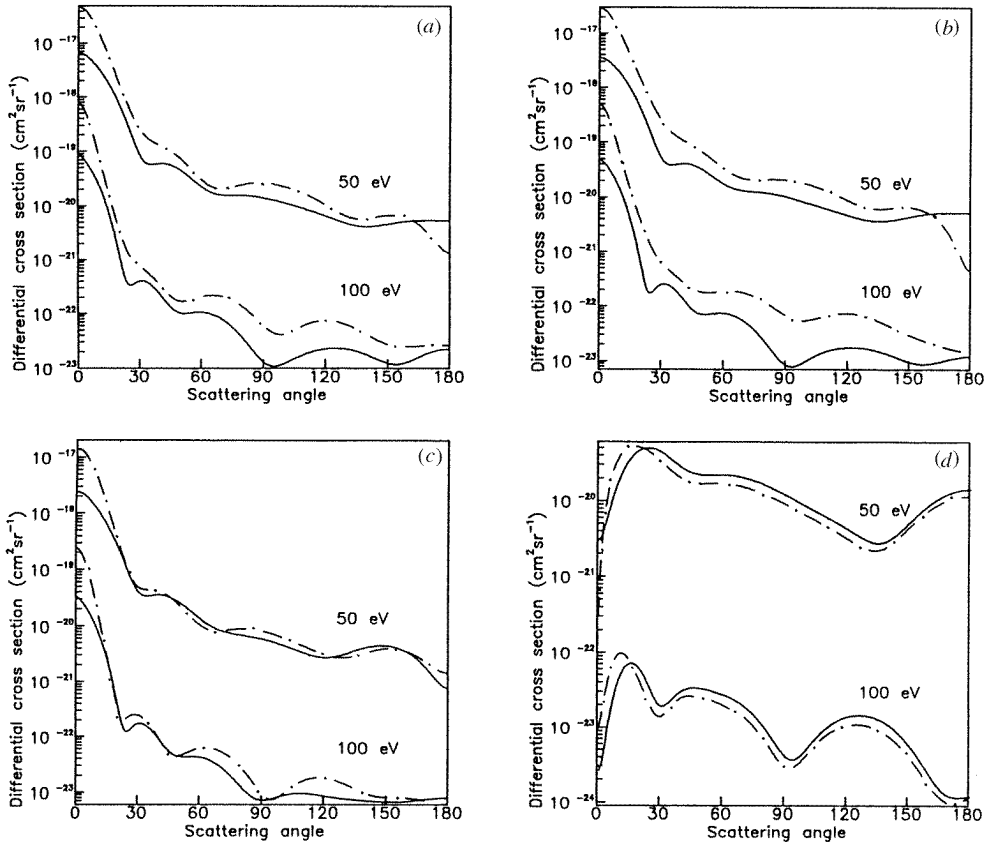

Figure 8. Same as figure 7 but for different $4p^5 5p$ $J_b = 2, 3$ states in Kr: (*a*) $5p[\frac{5}{2}]_2$, (*b*) $5p'[\frac{3}{2}]_2$, (*c*) $5p[\frac{3}{2}]_2$ and (*d*) $5p[\frac{5}{2}]_3$.

R-matrix calculations of Nakazaki *et al* (1997) which are available at 15 and 20 eV. From figure 9, we see, as pointed out by Khakoo *et al* (1996), that their results are lower that those of Filipović *et al* (1988). Furthermore, our SCGS and MCGS calculations are in reasonable agreement with the experimental data. However, the MCGS results are in better quantitative agreement with the experimental data of Khakoo *et al* (1996). They also agree well with the FOMBT data for small scattering angles. Nonetheless, it can be seen that no theory fully reproduces the experiment. In figures 10 and 11, we show our DCS results for the excitation of the $5p^5 6p$, $J_b = 1, 2$ and 3 states at 50 and 80 eV and compare them with the FOMBT data (Fontes *et al* 1997). There is relatively good agreement between the shape of the FOMBT data and our SCGS results though the FOMBT data are generally larger in magnitude.

3.2. Total cross sections

In figures 12 and 13 we present our total cross section (TCS) results for the excitation of the $3p^5 4p$, $J_b = 1, 2$ and 3 states of argon and compare them with other experimental and theoretical values. In figure 12 we compare our TCS for the $4p[\frac{1}{2}]_1$, $4p'[\frac{1}{2}]_1$, $4p[\frac{3}{2}]_1$ and $4p'[\frac{3}{2}]_1$ states with the non-relativistic theory of Bubelev and Grum-Grzhimailo (1991), the

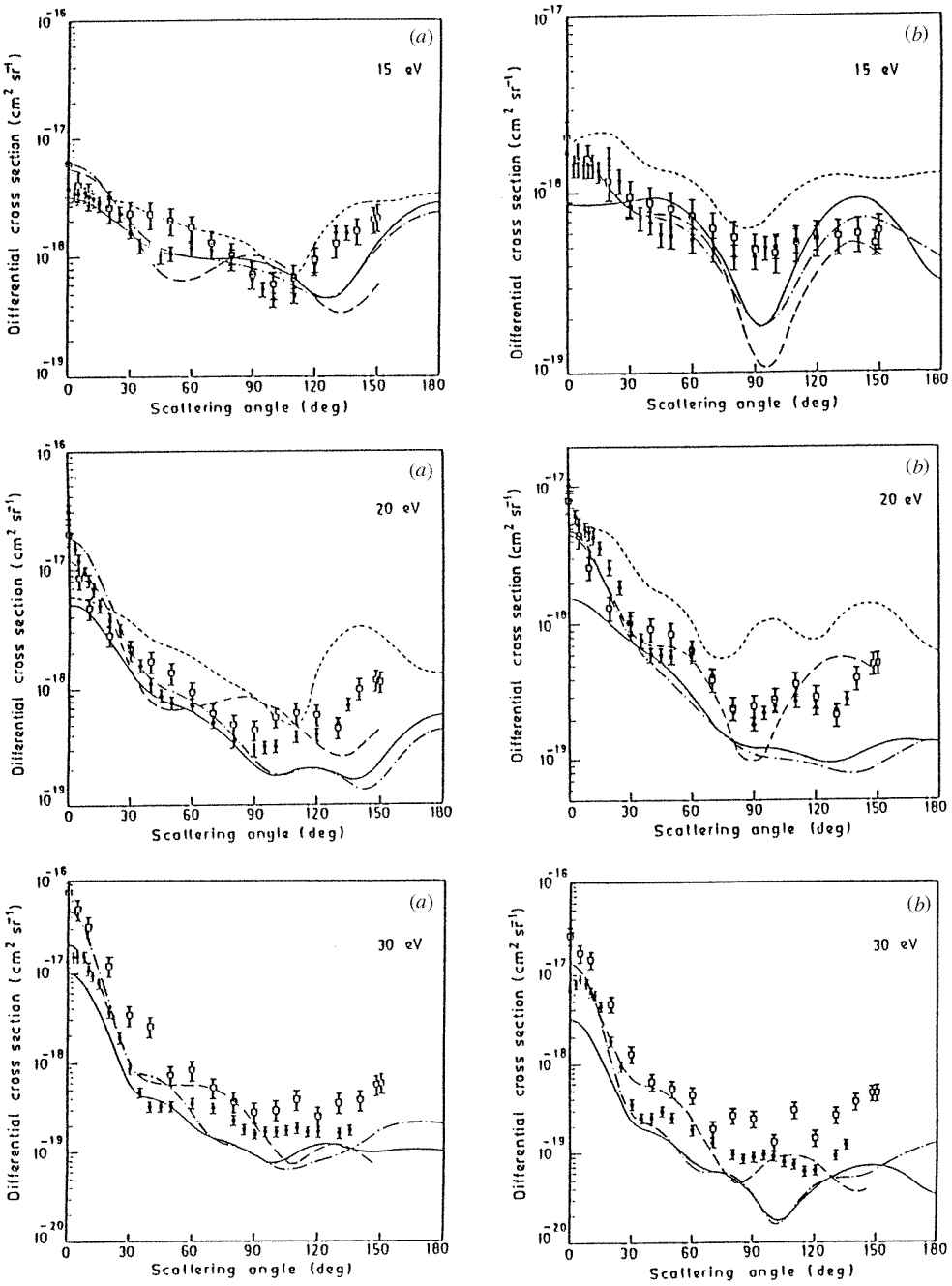

Figure 9. Comparison of the DCS with experiment for the excitation of Xe to (*a*) the unresolved $6p[\frac{5}{2}]_2 + 6p[\frac{5}{2}]_3$ states and (*b*) the unresolved $6p[\frac{3}{2}]_1 + 6p[\frac{3}{2}]_2$ states at 15, 20 and 30 eV. Theory: ——, present SCGS results; — · —, present MCGS results; - - - -, semi-relativistic *R*-matrix results of Nakazaki *et al* (1997); – – –, FOMBT results of Khakoo *et al* (1996). Experiment: ●, Khakoo *et al* (1996); □, Filipović *et al* (1988).

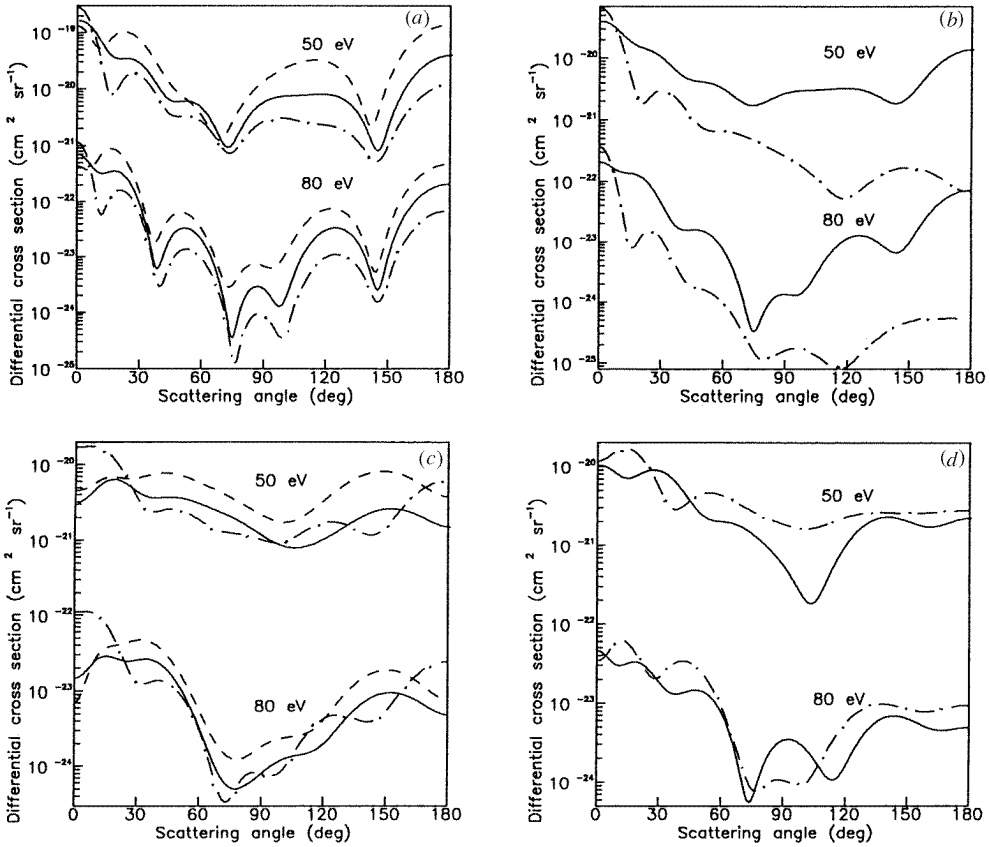

Figure 10. The DCS results for the excitation of different $5p^5 6p$ $J_b = 1$ states in Xe: (*a*) $6p[\frac{1}{2}]_1$, (*b*) $6p'[\frac{1}{2}]_1$, (*c*) $6p[\frac{3}{2}]_1$ and (*d*) $6p'[\frac{3}{2}]_1$. (Note that the values at 80 eV have been divided by 100.) Theory: ——, present SCGS results; — · —, present MCGS results. – – –, FOMBT results.

semi-relativistic distorted-wave theory of Madison *et al* (1998) and the experimental data of Chutjian and Cartwright (1981), Bogdanova and Yurgenson (1987) and Chilton *et al* (1998). From this figure, we see that the results of Bubelev and Grum-Grzhimailo (1991) have similar behaviour to our RDW theory but are slightly different in magnitude. The data of Chutjian and Cartwright (1981) are closer to the theoretical results than those of Bogdanova and Yurgenson (1987) or Chilton *et al* (1994), with the agreement being better at lower energies. Our MCGS results are in better agreement with experiment for the $4p'[\frac{3}{2}]_1$ and $4p[\frac{3}{2}]_1$ states than for the $4p'[\frac{1}{2}]_1$ and $4p[\frac{1}{2}]_1$ states.

In figure 13 we make similar comparisons for the $4p[\frac{5}{2}]_2$, $4p'[\frac{3}{2}]_2$, $4p[\frac{3}{2}]_2$ and $4p[\frac{5}{2}]_3$ states of argon. Here the overall agreement between theory and experiment is better than in figure 12 which is consistent with our experience with the DCS. We also note that our MCGS results lie above the SCGS results for the $J_b = 2$ states and that the MCGS results agree with the experiments only at low and high energies. The MCGS results are close to the experimental data of Bogdanova and Yurgenson (1987) and Chilton *et al* (1998), whereas the SCGS results are in better agreement with the experiment of Chutjian and Cartwright

Table 3. Total cross section (in 10^{-16} cm^2) for various excited states in krypton.

eV	$5p'[3/2]_1$	$5p[1/2]_1$	$5p'[1/2]_1$	$5p[3/2]_1$	$5p[5/2]_2$	$5p'[3/2]_2$	$5p[3/2]_2$	$5p[5/2]_3$
SCGS								
20	2.095(−3)[a]	4.863(−2)	2.185(−2)	1.566(−2)	2.961(−2)	2.622(−2)	2.569(−2)	3.980(−2)
30	8.114(−4)	9.711(−3)	4.106(−3)	2.910(−3)	1.785(−2)	1.139(−2)	8.997(−3)	8.193(−3)
40	4.040(−4)	4.385(−3)	1.741(−3)	1.120(−3)	1.452(−2)	8.604(−3)	6.186(−3)	3.416(−3)
50	2.303(−4)	2.629(−3)	9.713(−4)	5.803(−4)	1.262(−2)	7.330(−3)	5.060(−3)	1.867(−3)
60	1.440(−4)	1.616(−3)	5.660(−4)	3.250(−4)	1.121(−2)	6.446(−3)	4.343(−3)	1.104(−3)
80	6.813(−5)	6.405(−4)	2.092(−4)	1.135(−4)	9.072(−3)	5.189(−3)	3.411(−3)	4.340(−4)
100	3.827(−5)	2.995(−4)	9.306(−5)	4.751(−5)	7.574(−3)	4.335(−3)	2.822(−3)	2.012(−4)
MCGS								
20	1.577(−2)	2.480(−2)	3.973(−3)	1.135(−2)	4.297(−2)	2.908(−2)	2.395(−2)	3.480(−2)
30	3.022(−3)	4.454(−3)	7.006(−4)	2.229(−3)	5.282(−2)	3.555(−2)	1.594(−2)	7.048(−3)
40	1.208(−3)	1.868(−3)	2.788(−4)	9.267(−4)	5.247(−2)	3.586(−2)	1.497(−2)	2.882(−3)
50	6.465(−4)	1.087(−3)	1.565(−4)	5.028(−4)	4.965(−2)	3.420(−2)	1.411(−2)	1.541(−3)
60	3.777(−4)	6.615(−4)	9.885(−5)	2.925(−4)	4.635(−2)	3.213(−2)	1.318(−2)	8.988(−4)
80	1.459(−4)	2.615(−4)	4.602(−5)	1.125(−4)	3.994(−2)	2.795(−2)	1.141(−2)	3.504(−4)
100	6.655(−5)	1.228(−4)	2.497(−5)	5.241(−5)	3.458(−2)	2.434(−2)	9.935(−3)	1.627(−4)

[a] The number in brackets denotes the power of ten by which the quantity is to be multiplied.

Table 4. Total cross section (in 10^{-16} cm^2) for various excited states in xenon.

eV	$6p'[3/2]_1$	$6p[1/2]_1$	$6p'[1/2]_1$	$6p[3/2]_1$	$6p[5/2]_2$	$6p'[3/2]_2$	$6p[3/2]_2$	$6p[5/2]_3$
SCGS								
20	1.755(−3)[a]	3.834(−2)	1.920(−2)	1.119(−2)	3.861(−2)	2.171(−2)	2.184(−2)	3.038(−2)
30	7.837(−4)	1.292(−2)	5.688(−2)	2.887(−3)	3.261(−2)	1.407(−2)	1.250(−2)	8.901(−3)
40	4.394(−4)	2.198(−3)	1.064(−3)	6.012(−4)	2.657(−2)	1.029(−2)	8.626(−3)	2.373(−3)
50	2.714(−4)	1.131(−3)	5.279(−4)	2.794(−4)	2.171(−2)	8.215(−3)	6.913(−3)	1.174(−3)
60	1.772(−4)	8.040(−3)	3.609(−4)	1.725(−4)	1.884(−2)	7.155(−3)	6.004(−3)	7.422(−4)
80	8.422(−5)	4.600(−4)	1.983(−4)	8.344(−5)	1.527(−2)	5.892(−3)	4.879(−3)	3.820(−4)
100	4.477(−5)	2.551(−4)	1.076(−4)	4.222(−5)	1.281(−2)	4.998(−3)	4.098(−3)	2.064(−4)
MCGS								
20	1.196(−2)	2.065(−2)	3.146(−3)	9.351(−3)	8.070(−2)	3.764(−2)	2.806(−2)	2.733(−2)
30	3.799(−3)	7.157(−3)	1.301(−3)	2.336(−3)	8.951(−2)	4.223(−2)	2.582(−2)	7.499(−3)
40	8.924(−4)	1.196(−3)	2.389(−4)	5.407(−4)	8.881(−2)	4.521(−2)	2.382(−2)	2.089(−3)
50	4.165(−4)	5.924(−4)	1.198(−4)	2.812(−4)	7.886(−2)	4.181(−2)	2.130(−2)	1.023(−3)
60	2.530(−4)	3.958(−4)	7.392(−5)	1.850(−4)	7.049(−2)	3.789(−2)	1.934(−2)	6.334(−4)
80	1.272(−4)	2.116(−4)	3.506(−5)	9.342(−5)	5.837(−2)	3.181(−2)	1.638(−2)	3.159(−4)
100	6.953(−5)	1.152(−4)	1.920(−5)	4.911(−5)	4.973(−2)	2.737(−2)	1.412(−2)	1.685(−4)

[a] The number in brackets denotes the power of ten by which the quantity is to be multiplied.

(1980).

Finally, in tables 3 and 4 we present our SCGS and MCGS values for the TCS at some selected energies for krypton and xenon since there are no other theoretical calculations or sufficient experimental data for comparison. However, we note that experimental data for the TCS for the excitation of the $5p\left[\frac{1}{2}\right]_1$ and the unresolved $5p\left[\frac{5}{2}\right]_2 + 5p\left[\frac{5}{2}\right]_3$ and $5p\left[\frac{3}{2}\right]_1 + 5p\left[\frac{3}{2}\right]_2$ states of krypton were reported by Trajmar *et al* (1981). Furthermore, the experimental data for the excitation of the unresolved $6p\left[\frac{5}{2}\right]_2 + 6p\left[\frac{5}{2}\right]_3$ and $6p\left[\frac{3}{2}\right]_1 + 6p\left[\frac{3}{2}\right]_2$

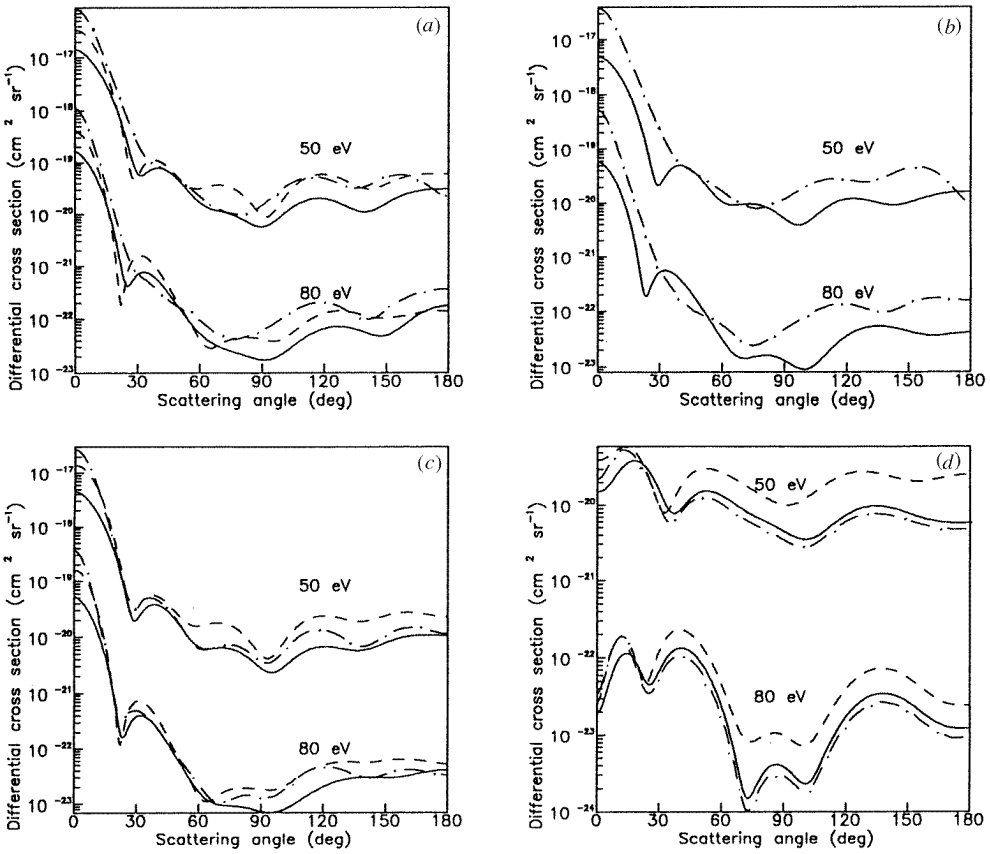

Figure 11. Same as figure 10 but for different $5p^5 6p$ $J_b = 2, 3$ states in Xe: (*a*) $6p[\frac{5}{2}]_2$, (*b*) $6p'[\frac{3}{2}]_2$, (*c*) $6p[\frac{3}{2}]_2$ and (*d*) $6p[\frac{5}{2}]_3$.

states of xenon were given by Filipović *et al* (1988) but only for a few energies near threshold. In general, our calculations were in good agreement with these data.

4. Conclusions

The RDW method, like most other distorted-wave methods, is a first-order theory and therefore can be expected to produce reliable results for direct excitations at higher energies. The strength of the distorted-wave methods is that they are more reliable at lower energies than simple first-order theories such as the first Born approximation. Nevertheless, experience has shown that its reliability often deteriorates at scattering energies below 30 eV. We would also expect less reliable results from distorted-wave calculations of excitations which proceed purely via an exchange interaction.

Our RDW results differ from other distorted-wave calculations quoted in this paper by being fully relativistic; that is, we use Dirac–Fock wavefunctions for the bound states which are based on the j–j coupling scheme and produce distinct energy values for the various fine-structure levels of the atom. The non- or semi-relativistic calculations use LS coupling

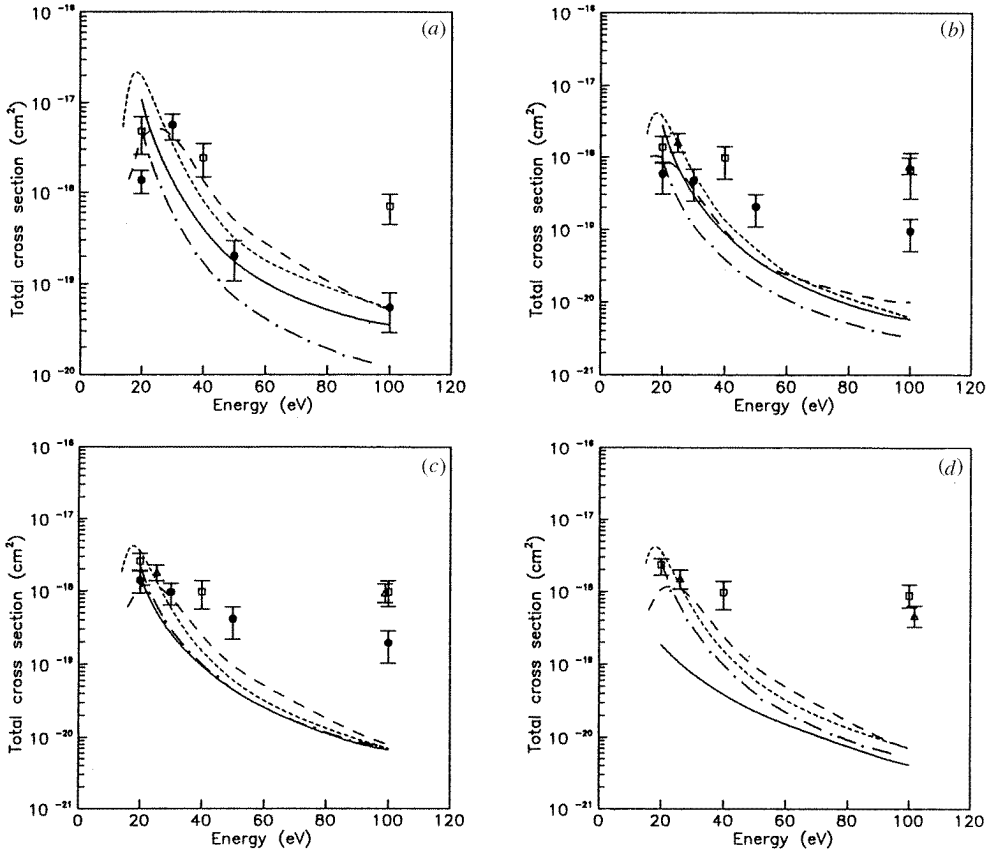

Figure 12. Comparison of the TCS with experiment for the excitation of different $3p^5 4p$ $J_b = 1$ states in Ar: (*a*) $4p[\frac{1}{2}]_1$, (*b*) $4p'[\frac{1}{2}]_1$, (*c*) $4p[\frac{3}{2}]_1$ and (*d*) $4p'[\frac{3}{2}]_1$. Theory: ——, present SCGS results; — · —, present MCGS results; - - - -, SRDW results of Madison *et al* (1998); – – –, DWA results of Bubelev and Grum-Grzhimailo (1991). Experiment: △, Bogdanova and Yurgenson (1987); ●, Chutjian and Cartwright (1981); □, Chilton *et al* (1998).

to calculate the various bound-state orbitals which are then recoupled to give wavefunctions for the various excited states. Thus all the fine-structure levels belonging to a given LS configuration have the same energy in this approach. One would not expect these different methods to yield vastly different results for a light atom like argon. But for heavier atoms like xenon, these differences can become important.

However, there are other important differences between our RDW method and both the SRDW method of Madison *et al* (1998) and the FOMBT of Khakoo *et al* (1996). We include the effects of exchange for the scattered electron via antisymmetrization of the total wavefunctions. Both of the other methods approximate this effect by means of a local exchange operator. This difference will be most apparent for excitations which are pure exchange processes. Moreover, the FOMBT method uses the initial-state interaction to calculate the distorted waves in both channels, while both Madison *et al* and the present work use the final-state interaction. Some idea of the effect of this can be gained by looking at the difference between the FOMBT and DWA results in Khakoo *et al*. The latter approximation uses different interaction potentials in the initial and final channels.

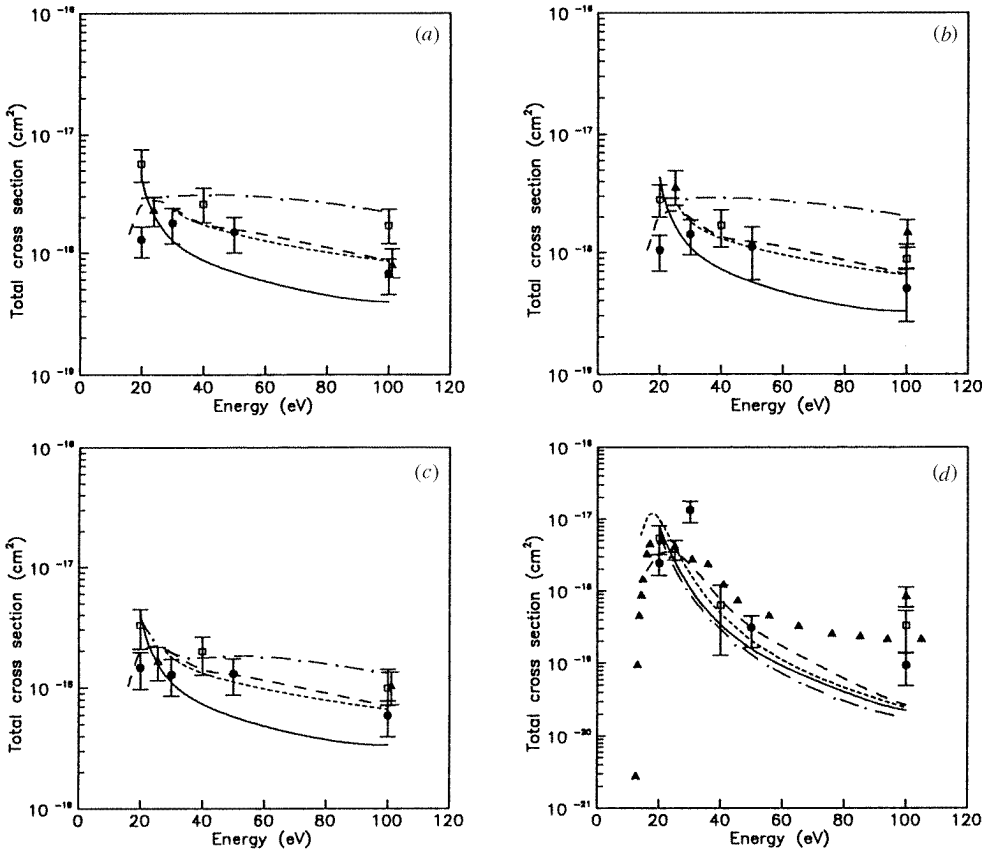

Figure 13. Same as figure 12 but for different $3p^5 4p$ $J_b = 2$, 3 states in Ar: (*a*) $4p[\frac{5}{2}]_2$, (*b*) $4p'[\frac{3}{2}]_2$, (*c*) $4p[\frac{3}{2}]_2$ and (*d*) $4p[\frac{5}{2}]_3$. Experiment: ▲, Gay *et al* (1996).

We should also add that *R*-matrix theories which are based on an expansion over a finite set of bound-state wavefunctions are most reliable at lower energies. Their reliability deteriorates at higher energies where there are a large or infinite number of open channels.

Turning to the experimental results, we note that the measurements of Chutjian and Cartwright (1981) were made in the angular range of 5–138°. They reported extrapolated results for argon for angles from 0–180° which we have included in our figures. However, the authors note that these extrapolated results are subject to additional errors beyond the experimental error bars.

As noted earlier, the excitation of the various $J_b = 2$ states can occur via a direct interaction as well as via exchange. For the $J_b = 1$ and 3 states, excitation can only occur via exchange. The DCS for direct excitations are characterized by a strong forward peak and generally larger values than those for exchange transitions. The theoretical cross sections for these exchange transitions are relatively flat in the forward direction with the notable exception of the $np[\frac{1}{2}]_1$ states.

If we examine our results in light of the above discussion we would expect the best agreement for the $J_b = 2$ states. This is indeed the case. For argon (figures 3 and 4(*a*)) our SCGS results agree closely in shape with the SRDW results of Madison *et al* and these two sets of calculations approach each other in magnitude as the energy increases. There is good

agreement between experiment and these theoretical results if one ignores the experimental results above 138°. The SCGS and MCGS results have a similar shape and the MCGS results are always higher in the small angle range. This latter behaviour holds for krypton (figure 8) and xenon (figure 11) as well.

In figures 5(*b*) and 6 (krypton) and figure 9 (xenon) the experimental measurements are a combination of the cross sections for the excitation of a $J_b = 1$ and 2 state. As can be seen from our calculations at higher energies, the cross section for the direct transition will dominate that for the exchange transition, at least for small angles. We also note that the agreement between theory and experiment is quite good for krypton and reasonable for xenon. In most cases, the MCGS results would seem to be more reliable in the forward direction for these heavier atoms.

Turning to the excitation of the $J_b = 1$ and 3 results, we note there is somewhat more variation between SCGS and MCGS results for these exchange transitions than for the direct transitions. This is not too surprising in light of the above discussion. For argon, we can compare our results for these transitions to the SRDW results of Madison *et al* and note there is close agreement with our SCGS results for the $4p[\frac{1}{2}]_1$, $4p[\frac{3}{2}]_1$ and $4p[\frac{5}{2}]_3$ states but considerable differences for the $4p'[\frac{1}{2}]_1$ and $4p'[\frac{3}{2}]_1$ states. Referring to table 1 we see that the former states correspond primarily to the excitation of a 3p electron to the $n = 4$ level, while the latter states correspond to the excitation of a $3\bar{p}$ electron in the j–j coupling scheme. Since Madison *et al* use the LS coupling scheme they have a single p orbital for each n level. Thus it appears that for these exchange transitions, there is a noticeable difference between the use of relativistic and non-relativistic bound-state orbitals. Alternatively, these differences could arise from the different treatment of exchange in these two calculations, as noted above.

The agreement with experiment is less satisfactory for the exchange transitions than for the direct ones. Somewhat surprisingly, all of the experimental cross sections show a strong forward peak, while the theoretical ones are relatively flat in this region with the exception of the $np[\frac{1}{2}]_1$ transitions. The other states for which experimental results are available, the $4p'[\frac{1}{2}]_1$, $4p[\frac{3}{2}]_1$ and $4p[\frac{5}{2}]_3$ states of argon, have an energy difference from a nearby $J_b = 2$ state which is comparable to the quoted energy spread of the experimental electron beam. Given that the theoretical cross sections are at least an order of magnitude greater for the direct transitions in this angular range, thus if even a small part of the signal attributed to the exchange transition comes from the nearby direct transition, this would cause large errors in the experimental results. Thus we must question the accuracy of the experimental results in the forward direction for these cases.

The TCS will reflect the behaviour of the DCS discussed above. In particular, the agreement between theory and experiment is best for the $J_b = 2$ states. All the theoretical results predict the same general behaviour with energy but there are larger differences between them for the direct transitions than for the exchange transitions. For the direct transitions, the forward peak in the DCS gives the majority of the contribution to the TCS so differences in the theoretical results in this angular range are reflected in differences in the TCS. Although there is less good agreement in shape among the theoretical DCS for the exchange transitions, the good agreement in the TCS indicates that the overall magnitude of these DCS has the same behaviour with energy.

In summary, the distorted-wave methods are most reliable for direct transitions. For these cases, the agreement between the various theories and with experiment is generally good. This reflects our previous experience with the RDW method. For exchange transitions, the results are very sensitive to the specific approximations made in the various

theoretical methods and the experimental measurements may suffer from systematic errors as well. Clearly more investigation is needed for these cases.

Acknowledgments

We are grateful to the Computer Centre, University of Roorkee for providing us with their computational facilities. The author (RS) is thankful to the University Grants Commission (UGC), New Delhi, India for financial assistance for this work. One of us (SK) is also thankful to the Council of Scientific and Industrial Research (CSIR), New Delhi, India for the award of a Senior Research Fellowship and research grant. Two of us (RPM and ADS) wish to thank the Natural Sciences and Engineering Research Council of Canada for financial support. We also wish to extend our thanks to Dr C Fontes, Professor D H Madison, Dr S Nakazaki and Dr V Zeman for sending us their numerical data in advance of publication.

References

Ballou J K, Lin Chun C and Fajen F E 1973 *Phys. Rev.* A **8** 1797
Bogdanova I P and Yurgenson S V 1987 *Opt. Spektrosk.* **62** 471
Bubelev V E and Grum-Grzhimailo A N 1991 *J. Phys. B: At. Mol. Opt. Phys.* **24** 2183
Chilton J E, Bofford J B, Shappe R S and Lin C C 1998 *Phys. Rev.* A **57** 267
Chutjian A and Cartwright D C 1981 *Phys. Rev.* A **23** 2178
Ester T and Kessler J 1994 *J. Phys. B: At. Mol. Opt. Phys.* **27** 4295
Filipović D, Marinković B, Pejčev V and Vušković L 1988 *Phys. Rev.* A **37** 356
Fontes C J *et al* 1997 *Differential Cross Sections for Electron Impact Excitation of the Twenty Lowest Levels of Xe: Experiment and Theory Report* LA-UR-96-4461 Los Alamos National Laboratory, Los Alamos, NM
Gay T J, Furst J E, Trantham K W and Wijayaratna W M K P 1996 *Phys. Rev.* A **53** 1623
Grant I P 1970 *Adv. Phys.* **19** 747
Grant I P, McKenzie B J, Norrington P H, Mayers D F and Piper N C 1980 *Comput. Phys. Commun.* **21** 207
Kaur S, Srivastava R, McEachran R P and Stauffer A D 1998 *J. Phys. B: At. Mol. Opt. Phys.* **31** 157
Khakoo M A, Trajmar S, Wang S, Kanik I, Aguirre A, Fontes C J, Clark R E H and Abdallah J 1996 *J. Phys. B: At. Mol. Opt. Phys.* **29** 3477
Madison D H, Maloney C M and Wang J B 1998 *J. Phys. B: At. Mol. Opt. Phys.* **31** 873
Moore C E 1971 *Atomic Energy Levels, National Standard Reference Data Series* vol 35 (Washington, DC: US Govt Printing Office)
Nakazaki S, Berrington K A, Eissner W B and Itikawa Y 1997 Private communication
Register D F, Vušković L and Trajmar S 1986 *J. Phys. B: At. Mol. Phys.* **19** 1685
Trajmar S, Srivastava S K, Tanaka H, Nishimura H and Cartwright D C 1981 *Phys. Rev.* A **23** 2167
Zeman and Bartschat Private communication